THE UNIVERSITY OF
WARWICK

Original citation:
NEMO-3 Collaboration (Including: Morgan, B. (Ben) and Ramachers, Yorke). (2014)
Search for neutrinoless double-beta decay of Mo100 with the NEMO-3 detector.
Physical Review D (Particles, Fields, Gravitation and Cosmology), Volume 5 (Number
89). Article number 111101.

Permanent WRAP url:
http://wrap.warwick.ac.uk/62163

warwick**publications**wrap

highlight your research

http://wrap.warwick.ac.uk/

Search for Neutrinoless Double-Beta Decay of ^{100}Mo with the NEMO-3 Detector

R. Arnold,[1] C. Augier,[2] J.D. Baker[†],[3] A.S. Barabash,[4] A. Basharina-Freshville,[5] S. Blondel,[2] S. Blot,[6]
M. Bongrand,[2] V. Brudanin,[7] J. Busto,[8] A.J. Caffrey,[3] C. Cerna,[9] A. Chapon,[10] E. Chauveau,[6] D. Duchesneau,[11]
D. Durand,[10] V. Egorov,[7] G. Eurin,[2,5] J.J. Evans,[6] R. Flack,[5] X. Garrido,[2] H. Gómez,[2] B. Guillon,[10]
P. Guzowski,[6] R. Hodák,[12] P. Hubert,[9] C. Hugon,[9] S. Jullian,[2] A. Klimenko,[7] O. Kochetov,[7] S.I. Konovalov,[4]
V. Kovalenko,[7] D. Lalanne,[2] K. Lang,[13] Y. Lemière,[10] Z. Liptak,[13] P. Loaiza,[14] G. Lutter,[9] F. Mamedov,[12]
C. Marquet,[9] F. Mauger,[10] B. Morgan,[15] J. Mott,[5] I. Nemchenok,[7] M. Nomachi,[16] F. Nova,[13] F. Nowacki,[1]
H. Ohsumi,[17] R.B. Pahlka,[13] F. Perrot,[9] F. Piquemal,[9,14] P. Povinec,[18] Y.A. Ramachers,[15] A. Remoto,[11]
J.L. Reyss,[19] B. Richards,[5] C.L. Riddle,[3] E. Rukhadze,[12] R. Saakyan,[5] X. Sarazin,[2] Yu. Shitov,[7,20]
L. Simard,[2,21] F. Šimkovic,[18] A. Smetana,[12] K. Smolek,[12] A. Smolnikov,[7] S. Söldner-Rembold,[6] B. Soulé,[9]
I. Štekl,[12] J. Suhonen,[22] C.S. Sutton,[23] G. Szklarz,[2] J. Thomas,[5] V. Timkin,[7] S. Torre,[5] Vl.I. Tretyak,[24]
V.I. Tretyak,[7] V.I. Umatov,[4] I. Vanushin,[4] C. Vilela,[5] V. Vorobel,[25] D. Waters,[5] and A. Žukauskas[25]

(NEMO-3 Collaboration)

^{1}IPHC, ULP, CNRS/IN2P3, F-67037 Strasbourg, France
^{2}LAL, Univ Paris-Sud, CNRS/IN2P3, F-91405 Orsay, France
^{3}Idaho National Laboratory, Idaho Falls, ID 83415, U.S.A.
^{4}ITEP, 117218 Moscow, Russia
^{5}UCL, London WC1E 6BT, United Kingdom
^{6}University of Manchester, Manchester M13 9PL, United Kingdom
^{7}JINR, 141980 Dubna, Russia
^{8}CPPM, Université de Marseille, CNRS/IN2P3, F-13288 Marseille, France
^{9}CENBG, Université de Bordeaux, CNRS/IN2P3, F-33175 Gradignan, France
^{10}LPC Caen, ENSICAEN, Université de Caen, CNRS/IN2P3, F-14050 Caen, France
^{11}LAPP, Université de Savoie, CNRS/IN2P3, F-74941 Annecy-le-Vieux, France
^{12}Institute of Experimental and Applied Physics, Czech Technical University in Prague, CZ-12800 Prague, Czech Republic
^{13}University of Texas at Austin, Austin, TX 78712, U.S.A.
^{14}Laboratoire Souterrain de Modane, F-73500 Modane, France
^{15}University of Warwick, Coventry CV4 7AL, United Kingdom
^{16}Osaka University, 1-1 Machikaney arna Toyonaka, Osaka 560-0043, Japan
^{17}Saga University, Saga 840-8502, Japan
^{18}FMFI, Comenius Univ., SK-842 48 Bratislava, Slovakia
^{19}LSCE, CNRS, F-91190 Gif-sur-Yvette, France
^{20}Imperial College London, London SW7 2AZ, United Kingdom
^{21}Institut Universitaire de France, F-75005 Paris, France
^{22}Jyväskylä University, FIN-40351 Jyväskylä, Finland
^{23}MHC, South Hadley, Massachusetts 01075, U.S.A.
^{24}Institute for Nuclear Research, MSP 03680, Kyiv, Ukraine
^{25}Charles University in Prague, Faculty of Mathematics and Physics, CZ-12116 Prague, Czech Republic
(Dated: June 24, 2014)

We report the results of a search for the neutrinoless double-β decay ($0\nu\beta\beta$) of ^{100}Mo, using the NEMO-3 detector to reconstruct the full topology of the final state events. With an exposure of 34.7 kg·y, no evidence for the $0\nu\beta\beta$ signal has been found, yielding a limit for the light Majorana neutrino mass mechanism of $T_{1/2}(0\nu\beta\beta) > 1.1 \times 10^{24}$ years (90% C.L.) once both statistical and systematic uncertainties are taken into account. Depending on the Nuclear Matrix Elements this corresponds to an upper limit on the Majorana effective neutrino mass of $\langle m_\nu \rangle < 0.3 - 0.9$ eV (90% C.L.). Constraints on other lepton number violating mechanisms of $0\nu\beta\beta$ decays are also given. Searching for high-energy double electron events in all suitable sources of the detector, no event in the energy region [3.2-10] MeV is observed for an exposure of 47 kg·y.

PACS numbers: 23.40.-s; 14.60.Pq

Many extensions of the Standard Model provide a natural framework for neutrino masses and lepton number violation. In particular the see-saw mechanism [1], which requires the existence of a Majorana neutrino, naturally explains the smallness of neutrino masses. The existence of Majorana neutrinos would also provide a natural framework for the leptogenesis process [2] which could explain the observed baryon-antibaryon asymmetry in the Universe. The observation of neutrinoless double-β decay

---

†Deceased

($0\nu\beta\beta$) would prove that neutrinos are Majorana particles [3] and that lepton number is not conserved. The isotopes for which a single-β is energetically forbidden or strongly suppressed are most suitable for the search of this rare radioactive process. The experimental signature of $0\nu\beta\beta$ decays is the emission of two electrons with total energy (E_{TOT}) equal to the Q-value of the decay ($Q_{\beta\beta}$).

The NEMO-3 experiment searches for the double-β decay of seven isotopes by reconstructing the full topology of the final state events. The NEMO-3 detector [4], installed in the Modane underground laboratory (LSM, France) under a rock overburden of 4800 m.w.e., ran between February 2003 and January 2011. Here we report on the results obtained with ^{100}Mo, the largest sample in NEMO-3, with a mass of 6914 g and $Q_{\beta\beta} = 3034.40 \pm 0.17$ keV [5]. The most stringent previously published bound on the half-life of the $0\nu\beta\beta$ decay of ^{100}Mo was obtained by NEMO-3 using a subset of the data sample analysed here, placing a limit $T > 4.6 \times 10^{23}$ y at 90% C.L.[6].

The distinctive feature of the NEMO-3 detection method is the full reconstruction with 3D-tracking and calorimetric information of the topology of the final state, comprising two electrons simultaneously emitted from a common vertex in a $\beta\beta$ source. The NEMO-3 detector consists of 20 sectors arranged in a cylindrical geometry containing thin (40-60 mg/cm^2) source foils of $\beta\beta$ emitters. The ^{100}Mo source foils were constructed from either a metallic foil or powder bound by an organic glue to mylar strips (composite foils). ^{100}Mo was purified through physical and chemical processes [4]. The foils are suspended between two concentric cylindrical tracking volumes consisting of 6180 drift cells operating in Geiger mode [4]. To minimize multiple scattering, the gaseous tracking detector is filled mainly with helium (95%) with admixtures of ethyl alcohol (4%), argon (1%) and water vapour (0.1%). The tracking detector is surrounded by a calorimeter made of large blocks of plastic scintillator (1940 blocks in total) coupled to low radioactivity 3" and 5" diameter photomultiplier tubes (PMTs). The tracking detector, immersed in a magnetic field, is used to identify electron tracks and can measure the delay time of any tracks up to 700 μs after the initial event. This is used to tag electron-alpha ($e^-\alpha$) events from the ^{214}Bi -^{214}Po cascade. The calorimeter measures the energy and the arrival time of the particles. For 1 MeV electrons the timing resolution is $\sigma = 250$ ps while the energy resolution is FWHM $= [14 - 17]\%/\sqrt{E(\text{MeV})}$. The detector response to the summed energy of the two electrons from the $0\nu\beta\beta$ signal is a peak broadened by the energy resolution of the calorimeter and fluctuations in electron energy losses in the source foils, which gives a non-Gaussian tail extending to low energies. The FWHM of the expected $0\nu\beta\beta$ two-electron energy spectrum for ^{100}Mo is 350 keV. Electrons and photons can be identified through tracking and calorimetry. A solenoid surrounding the detector produces a 25 G magnetic field to reject pair production and external electron events. The detector is shielded from external gamma rays by 19 cm of low activity iron and 30 cm of water with boric acid to suppress the neutron flux. A radon trapping facility was installed at the LSM in autumn 2004, reducing the radon activity of the air surrounding the detector. As a consequence, the radon inside the tracking chamber is reduced by a factor of about 6. The data taken by NEMO-3 are subdivided into two data sets hereafter referred to as Phase 1 (February 2003 − November 2004) and Phase 2 (December 2004 − December 2010), respectively. Results obtained with both data sets are presented here.

Twenty calibration tubes located in each sector near the source foils are used to introduce up to 60 radioactive sources (^{207}Bi, ^{232}U). The calorimeter absolute energy scale is calibrated every 3 weeks with ^{207}Bi sources which provide internal conversion electrons of 482 and 976 keV. The linearity of the PMTs was verified in a dedicated light injection test during the construction phase and deviation was found to be less than 1% in the energy range [0-4] MeV. The 1682 keV internal conversion electron peak of ^{207}Bi is used to determine the systematic uncertainty on the energy scale: the data-Monte Carlo disagreement in reconstructing the peak position is less than 0.2%. For 99% of the PMTs the energy scale is known with an accuracy better than 2%. Only these PMTs are used in the data analysis presented here. The relative gain and time variation of individual PMTs is surveyed twice a day by a light injection system; PMTs that show a gain variation of more than 5% compared to a linear interpolation between two successive absolute calibrations with ^{207}Bi are rejected from the analysis.
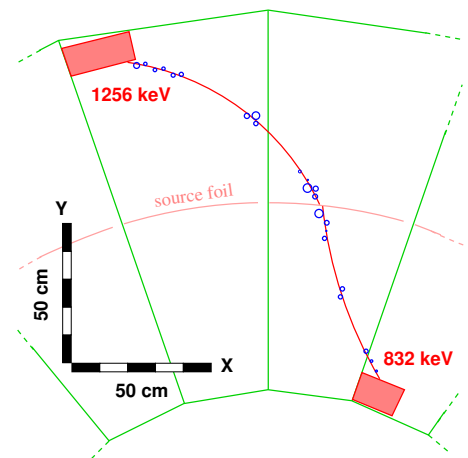
FIG. 1: Transverse view of a reconstructed $\beta\beta$ data event with a two electron energy sum of 2088 keV. Two tracks are reconstructed from a single vertex in the source foil, with an electron-like curvature in the magnetic field, and are each associated to an energy deposit in a calorimeter block.

Two-electron ($2e^-$) events are selected with the following requirements. Two tracks with a length greater than 50 cm and an electron-like curvature must be reconstructed. The geometrical efficiency is 28.3 %. Both

tracks are required to originate from a common reconstructed vertex in the ^{100}Mo source foil with transverse and longitudinal resolutions of $\sigma_t = [2-3]$ mm and $\sigma_l = [7-13]$ mm, respectively [4]. The tracks terminate in isolated scintillator blocks with a single energy deposit greater than 0.2 MeV. A time of flight criterion requires that the two electrons should be emitted from the source foil. There must be no photons or delayed tracks present in the event. Fig. 1 shows a candidate $\beta\beta$ event observed in the data.

When searching for rare processes, the background estimation is of paramount importance. An exhaustive program, described in detail in [7], has been carried out to measure the backgrounds in the NEMO-3 detector. The sources of backgrounds relevant to the $0\nu\beta\beta$ search in ^{100}Mo are the irreducible background from its $2\nu\beta\beta$ decay, as well as the decays of ^{214}Bi and ^{208}Tl originating from the natural decay chains of ^{238}U and ^{232}Th. These high-Q_β isotopes can produce $2e^-$ events by one of the following mechanisms: a β decay followed by a Møller scattering interaction, a β-γ cascade followed by a Compton scattering of the emitted γ close to the vertex or a β decay accompanied by emission of an internal conversion electron. The background isotopes can either be present in the $\beta\beta$ source foils, or can result from ^{222}Rn or ^{220}Rn emanation. The isotopes ^{214}Bi and ^{208}Tl are progenies of ^{222}Rn and ^{220}Rn respectively and can end up on the surfaces of the source foils and drift cell wires located in the vicinity of the foils.

The ^{100}Mo foil internal backgrounds are measured with the full statistics of the entire data set using topologies, energy and timing information specific for the background in question [7]. The results are summarized in Table I. The ^{214}Bi activity inside the source foils and from ^{222}Rn is measured with the $1e^-\alpha$ delayed coincidence channel which is an efficient and background free signature of the ^{214}Bi-^{214}Po β-α decay cascade. The total ^{222}Rn activity inside the 28 m^3 tracker chamber is measured to be 1138 ± 199 mBq and 205 ± 77 mBq in Phase 1 and Phase 2, respectively. The ^{220}Rn activity is found to be at a level of 3 mBq giving a negligible contribution to $2e^-$ events. The non-uniform distribution of the deposition of the Rn daughters inside the tracker is also taken into account [7]. The ^{214}Bi location inside the source foils, or on the surface of the foils and drift wires can be statistically separated by fitting the α track length distribution. The ^{208}Tl activity is measured with the $1e^-$ nγ channel (n$\geq$1), which contains events due to the β decay of ^{208}Tl followed by de-excitation γ-rays of the ^{208}Pb daughter isotope. The ^{214}Bi and ^{208}Tl contamination measurements are independently verified using the $2e^-$ + X event topologies in the energy range [2.8-3.2] MeV where a large part of the ^{100}Mo $0\nu\beta\beta$ signal is expected. For ^{214}Bi, 6 events with a $2e^-1\alpha$ topology are observed in the data after a total exposure of 34.7 kg·y while 9.4 ± 0.5 are expected from simulations. For ^{208}Tl, 7 events with a $2e^-$nγ topology are observed in the same data sample, while 8.8 ± 0.6 are expected. Both tests,

TABLE I: Foil contamination activities for the ^{100}Mo source measured by NEMO-3, and their contribution to the background in the $2e^-$ channel within the $E_{TOT} = [2.8$-$3.2]$ MeV range. The uncertainties are statistical only. The masses of ^{100}Mo from metallic and composite sources are respectively 2479 g and 4435 g.

| | ^{100}Mo metallic/composite | |
	Activities (μBq/kg)	Number of $2e^-$ events
^{214}Bi internal	$60 \pm 20/380 \pm 40$	$0.07 \pm 0.02/0.91 \pm 0.07$
^{208}Tl internal	$87 \pm 4/128 \pm 3$	$0.91 \pm 0.04/2.39 \pm 0.06$

although statistically limited, show that the prediction of the background contribution to $0\nu\beta\beta$ from ^{214}Bi and ^{208}Tl are reliable within the quoted uncertainties.

Neutrons produced by (α,n) reactions and spontaneous fission reactions are also a potential source of background. They can be thermalized in the scintillator material and subsequently captured producing γ-rays with energies up to 10 MeV. These high energy γ-rays can interact with the source foils and mimic $\beta\beta$ events through pair creation, double Compton scattering or a Compton scattering followed by a Møller interaction. A model of the neutron background is validated with dedicated runs using a calibrated Am-Be neutron source and is found to be negligible for the $0\nu\beta\beta$ search.

The radon and external background model are verified in the energy region close to the ^{100}Mo $Q_{\beta\beta}$-value by selecting $2e^-$ events from the sectors containing Cu, ^{130}Te and natural Te foils. The internal contamination of these foils with radioactive isotopes is independently measured. The $2\nu\beta\beta$ decay of ^{130}Te gives no contribution above 2.4 MeV [8]. With an exposure of 13.5 kg · y only 3 events with $2e^-$ from the sectors containing Cu, ^{130}Te and natural Te foils remain in the energy window [2.8-3.2] MeV in the full data set, compared to a MC expectation of 3.6 ± 0.2 events, dominated by radon background.

Another background to $0\nu\beta\beta$ decays is the $2\nu\beta\beta$ decay allowed in the Standard Model. There are 683,049 $2e^-$ events in the full energy range of $E_{TOT} = [0.4$ - $3.2]$ MeV with a signal-to-background ratio of 76. The $2\nu\beta\beta$ contribution is found by fitting the energy sum distribution of two electrons using the shape of the $2\nu\beta\beta$ spectrum predicted by the Single State Dominance model for ^{100}Mo [9], taking into account the backgrounds quoted previously. Figure 2 shows for $E_{TOT} > 2$ MeV the spectra of the $2e^-$ energy sum, exhibiting good agreement between the data and MC. The number of $2\nu\beta\beta$ events obtained from this fit with $E_{TOT} > 2$ MeV corresponds to a ^{100}Mo half-life of $T_{1/2}(2\nu\beta\beta) = [6.93 \pm 0.04 \text{ (stat)}] \times 10^{18}$ y, in agreement with the previously published result [6] and with [10].

Figure 2 shows the tail of the E_{TOT} distribution in the energy window $E_{TOT} = [2.8$-$3.2]$ MeV around the $Q_{\beta\beta}$-value of ^{100}Mo $0\nu\beta\beta$ decay. The background contributions in this energy window are shown in Table II. No events are observed in the region of $E_{TOT} = [3.2$-$10]$ MeV
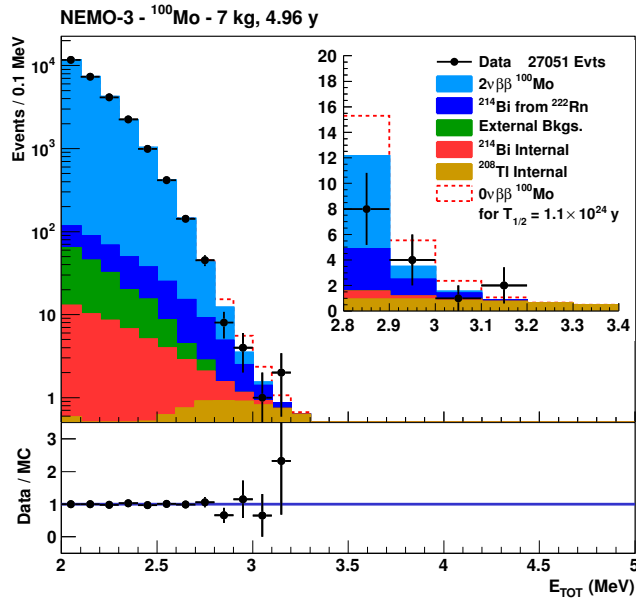
FIG. 2: Distribution of the two-electron energy sum, E_{TOT} and the ratio between the observed and the expected distributions from Monte Carlo simulations. The distribution is for $E_{TOT} > 2$ MeV and is obtained with an exposure of 34.7 kg·y. The solid histogram represents the expected spectrum consisting of $2\nu\beta\beta$ decays and radioactive backgrounds determined by Monte Carlo simulations. The dashed histogram in the E_{TOT} distribution represents a hypothetical $0\nu\beta\beta$ signal corresponding to a half-life of 1.1×10^{24} y.

TABLE II: Number of expected background and observed $2e^-$ events in Phase 1 and Phase 2 after a 34.7 kg·y exposure with ^{100}Mo in the $E_{TOT} = [2.8\text{-}3.2]$ MeV range. The $0\nu\beta\beta$ detection efficiency is 4.7% in this window.

Data sets	Phase 1	Phase 2	Combined
External background	< 0.04	< 0.16	< 0.2
^{214}Bi from ^{222}Rn	2.8 ± 0.3	2.5 ± 0.2	5.2 ± 0.5
^{214}Bi internal	0.20 ± 0.02	0.80 ± 0.08	1.0 ± 0.1
^{208}Tl internal	0.65 ± 0.05	2.7 ± 0.2	3.3 ± 0.3
$2\nu\beta\beta$	1.28 ± 0.02	7.16 ± 0.05	8.45 ± 0.05
Total expected	4.9 ± 0.3	13.1 ± 0.3	18.0 ± 0.6
Data	3	12	15

for NEMO-3 sources containing isotopes with $Q_{\beta\beta}$-value below 3.2 MeV (^{100}Mo, ^{82}Se, ^{130}Te, ^{116}Cd) or without $\beta\beta$ emitter isotopes (Cu) during the entire running period, which corresponds to an exposure of 47 kg · y.

As no event excess is observed in the data above the background expectation, a limit on the $0\nu\beta\beta$ decay of ^{100}Mo is set. The systematic uncertainties that are used in setting the $0\nu\beta\beta$ limit have two main components, the uncertainty on the $0\nu\beta\beta$ detection efficiency and the uncertainties on the background contribution. The uncertainty on the signal efficiency is determined using dedicated runs with activity-calibrated ^{207}Bi sources and is found to be 7%. The systematic uncertainties on the

TABLE III: Limits at 90%C.L. on the half-lives of lepton number violating processes (in units of 10^{24} y).

$0\nu\beta\beta$ Process	Statistical only	With systematics	Expected with systematics (median, [-1 σ,+1 σ] range)
Mass mechanism	1.1	1.1	1.0 [0.7-1.4]
RH current $\langle\lambda\rangle$	0.7	0.6	0.5 [0.4-0.8]
RH current $\langle\eta\rangle$	1.0	1.0	0.9 [0.6-1.3]
Majoron	0.050	0.044	0.039 [0.027-0.059]

background contributions are due to the activities of $2\nu\beta\beta$, ^{214}Bi and ^{208}Tl. The uncertainty on $2\nu\beta\beta$ is obtained from the fit to $2e^-$ events above 2 MeV described above and is 0.7%. The uncertainty on the ^{214}Bi contribution from ^{222}Rn and internal foil contamination, estimated by comparing the activities of this isotope measured independently in $1e1\alpha$ and $1e1\gamma$ channels, is 10%. The uncertainty on the ^{208}Tl contamination is determined from dedicated runs with a calibrated ^{232}U source and is found to be 10%. As a result of these estimates, a systematic uncertainty of 10% on the background contribution from ^{214}Bi and ^{208}Tl radioactive impurities is assumed in setting the limit on the ^{100}Mo $0\nu\beta\beta$ decay.

The limit is set using a modified frequentist analysis that employs a log-likelihood ratio test statistic [11]. The method uses the full information of the binned energy sum distribution in the $E_{TOT} = [2.0\text{-}3.2]$ MeV energy range for signal and background (Figure 2), as well as the statistical and systematic uncertainties and their correlations as described in more detail in [11, 12]. The data are described well by the background-only hypothesis with $1\text{-CL}_b = 64.7$ %, where 1-CL_b is the p-value of the background-only hypothesis.

The $0\nu\beta\beta$ detection efficiency for ^{100}Mo in NEMO-3 is 11.3% for the energy sum of two electrons above 2 MeV. Taking into account the total exposure of 34.7 kg·y, a limit on the light Majorana neutrino mass mechanism for $0\nu\beta\beta$ decay of ^{100}Mo is set (Table III). The result agrees with the expected sensitivity of the experiment and is twice more stringent than the previous best limit for this isotope [6]. The corresponding upper limit on the effective Majorana neutrino mass is $\langle m_\nu \rangle < 0.3 - 0.9$ eV (90% C.L.), where the range is determined by existing uncertainties in the nuclear matrix element (NME) [13–17] and phase space [18, 19] calculations.

Constraints on other lepton number violating mechanisms of $0\nu\beta\beta$ are set. Right-left symmetric models can give rise to $0\nu\beta\beta$ due to the presence of right-handed currents in the electroweak Lagrangian. This mechanism leads to different angular and single energy distributions of the final state electrons and can therefore be distinguished from other mechanisms in a NEMO-like experiment [20]. The corresponding half-life limits are given in Table III and translate into an upper bound on the coupling between right-handed quark and lepton currents of $\langle\lambda\rangle < (0.9 - 1.3) \times 10^{-6}$ (90% C.L.); and into an upper

TABLE IV: Limits at 90% C.L. on the half-lives and lepton number violating parameters. $\langle m_\nu \rangle$ contraints, both experimental published values and recalculated from [13–17, 34] are shown.

Isotope	Half-life $(10^{25}$ y) published	$\langle m_\nu \rangle$ (eV) published	$\langle m_\nu \rangle$ (eV) recalculated	$\langle \lambda \rangle$ (10^{-6}) published	$\langle \eta \rangle$ (10^{-8}) published	λ'_{111}/f (10^{-2}) published	$\langle g_{ee} \rangle$ (10^{-5}) published
[100]Mo This Work	0.11	0.33-0.87	0.33-0.87	0.9-1.3[a]	0.5-0.8[a]	4.4-6.0	1.6-4.1[a]
[130]Te [27, 28]	0.28	0.3-0.71	0.31-0.75	1.6-2.4[b]	0.9-5.3[b]		17-33[c]
[136]Xe [29, 30]	1.9	0.14-0.34	0.14-0.34				0.8-1.6
[76]Ge [31]	2.1	0.2-0.4	0.26-0.62				
[76]Ge [32, 33]	1.9	0.35	0.27-0.65	1.1	0.64		8.1

[a] obtained with half-lives given in Table III, [b] using the half-life limit of 2.1×10^{23}y, [c] using the half-life limit of 2.2×10^{21}y.

bound on the coupling between right-handed quark and left-handed lepton currents of $\langle \eta \rangle < (0.5 - 0.8) \times 10^{-8}$ (90% C.L.). The constraints are obtained using the NME calculations from [21–23].

In supersymmetric models the $0\nu\beta\beta$ process can be mediated by a gluino or neutralino exchange. Using the above half-life limit and the NME from [24] an upper bound is obtained on the trilinear R-parity violating supersymmetric coupling of $\lambda'_{111} < (4.4 - 6.0) \times 10^{-2}$f, where $f = \left(\frac{M_{\tilde{q}}}{1\,\mathrm{TeV}} \right)^2 \left(\frac{M_{\tilde{g}}}{1\,\mathrm{TeV}} \right)^{1/2}$ and $M_{\tilde{q}}$ and $M_{\tilde{g}}$ represent the squark and the gluino masses.

Finally, the $0\nu\beta\beta$ decay can be accompanied by a light or massless boson that weakly couples to the neutrino, called a Majoron. In this case the energy sum of the two emitted electrons, E_{TOT}, will have a broad spectrum ranging from zero to $Q_{\beta\beta}$ of ^{100}Mo. The exact shape will depend on the spectral index n, which determines the phase space dependence on the energy released in the decay, $G^{0\nu} \propto (Q_{\beta\beta} - E_{\mathrm{TOT}})^n$. The lower bound on the half-life of the Majoron accompanied $0\nu\beta\beta$ decay with the spectral index $n = 1$ is given in Table III. This is almost a factor of two more stringent limit than the previous best limit for this isotope [25]. Taking into account the phase space factors given in [26] and

the NME calculated in [13–17], an upper bound on the Majoron-neutrino coupling constant has been obtained, $\langle g_{ee} \rangle < (1.6 - 4.1) \times 10^{-5}$.

All the obtained limits on the lepton number violating parameters are comparable with the best current results obtained with other isotopes, as shown in Table IV.

In summary, with an exposure of 34.7 kg·y, no evidence for the $0\nu\beta\beta$ decay of ^{100}Mo is found. Taking into account statistical and systematic uncertainties, the half-life limit for the light Majorana neutrino mass mechanism is $T_{1/2}(0\nu\beta\beta) > 1.1 \times 10^{24}$ years (90% C.L.). The corresponding limit on the effective Majorana neutrino mass is $\langle m_\nu \rangle < 0.3 - 0.9$ eV, depending on the nuclear matrix elements assumed. The absence of a constant background in the high energy part of the spectrum is an encouraging result for future $0\nu\beta\beta$ NEMO-3 like experiments that plan to use high $Q_{\beta\beta}$-value isotopes such as ^{48}Ca, ^{96}Zr and ^{150}Nd.

[1] P. Minkowski, Phys. Lett. B 67 (1977) 421; T. Yanagida, Prog. Theor. Phys. 64 (1980) 1103; M. Gell-Mann, P. Ramond and R. Slansky, Proceedings of the Supergravity Stony Brook Workshop, New York 1979, eds. P. Van Nieuwenhuizen and D. Freedman (North-Holland, Amsterdam, 1979); R. N. Mohapatra and G. Senjanovic, Phys. Rev. Lett. 44 (1980) 912.

[2] M. Fukugita and T. Yanagida, Phys. Lett. B 174 (1986) 45.

[3] J. Schechter and J.W.F. Valle, Phys. Rev. D 25 (1982) 2951.

[4] R. Arnold et al., Nucl. Inst. Meth. A 536 (2005) 79.

[5] S. Rahaman et al., Phys. Lett. B 662 (2008) 111.

[6] R. Arnold et al., Phys. Rev. Lett. 95 (2005) 182302.

[7] J. Argyriades et al., Nucl. Inst. Meth. A 606 (2009) 449.

[8] R. Arnold et al., Phys. Rev. Lett. 107 (2011) 062504.

[9] J. Abad, A. Morales, R. Nunez-Lagos and P. F. Pacheo,

Ann. Fis. A 80 (1984) 9; P. Domin et al., Nucl. Phys. A753 (2005) 337.

[10] Particle Data Group, J. Beringer et al., Phys. Rev. D 86 (2012) 010001.

[11] T. Junk, Nucl. Inst. Meth. A 434 (1999) 435.

[12] J. Argyriades et al., Phys. Rev. C 80 (2009) 032501.

[13] J. Suhonen and O. Civitarese, J. Phys. G 39 (2012) 124005.

[14] F. Šimkovic, V. Rodin, A. Faessler and P.Vogel, Phys. Rev. C 87 (2013) 045501.

[15] J. Barea and F. Iachello, Phys. Rev. C 79 (2009) 044301.

[16] P. K. Rath, R. Chandra, K. Chaturvedi, P. K. Raina and J.G. Hirsch, Phys. Rev. C 82 (2010) 064310.

[17] T.R. Rodriguez and G. Martinez-Pinedo, Phys. Rev. Lett. 105 (2010) 252503.

[18] J. Kotila and F. Iachello, Phys. Rev. C 85 (2012) 034316.

[19] S. Stoica and M. Mirea, Phys. Rev. C 88 (2013) 037303.

[20] R. Arnold et al., Eur. Phys. J. C 70 (2010) 927.
[21] J. Suhonen, Nucl. Phys. A 700 (2002) 649.
[22] T. Tomoda, Rept. Prog. Phys. 54 (1991) 53.
[23] K. Muto, E. Bender and H.V. Klapdor, Z. Phys. A 334 (1989) 187.
[24] A. Faessler, G.L. Fogli, E. Lisi, A.M. Rotunno and F. Šimkovic, Phys. Rev. D 83 (2011) 113015
[25] R. Arnold et al., Nucl. Phys. A 765 (2006) 483.
[26] M. Doi, T. Katani and E. Takasugi, Phys. Rev. C 37 (1988) 2104.
[27] E. Andreotti et al., Astropart. Phys. 34 (2011) 822.

[28] C. Arnaboldi et al, Phys. Lett. B 557 (2003) 167.
[29] A. Gando et al., Phys. Rev. Lett. 110 (2013) 062502.
[30] A. Gando et al., Phys. Rev. C 86 (2012) 021601.
[31] M. Agostini et al., Phys. Rev. Lett. 111 (2013) 122503.
[32] H. V. Klapdor Kleingrothaus et al., Eur. Phys. J A 12 (2001) 147.
[33] M. Günther et al., Phys. Rev. D 55 (1997) 54.
[34] J. Menendez, A. Poves, E. Caurier and F. Nowacki, Nucl. Phys. A 818 (2009) 139.